PROCEEDINGS OF SCIENCE

Rare radiative and semileptonic $\mathbf{b} \to \mathbf{s}\ell\ell$ decays at Belle

Simon Wehle*
DESY (Deutsches Elektronen-Synchrotron)
E-mail: simon.wehle@Desy.de

We present a measurement of angular observables and a test of lepton flavor universality in the $B \to K^*\ell\ell$ decay, where ℓ is either e or μ. For the first time, the angular analysis in the decay is performed separately for the electron and muon channels. The analysis is performed using a data sample corresponding to an integrated luminosity of 711 fb^{-1} that contains 772×10^6 $B\bar{B}$ pairs, collected at the $\Upsilon(4S)$ resonance with the Belle detector at the KEKB asymmetric-energy e^+e^- collider.

9th International Workshop on the CKM Unitarity Triangle
28 November - 3 December 2016
Tata Institute for Fundamental Research (TIFR), Mumbai, India

*Speaker.

PoS(CKM2016)073

1. Introduction

Rare decays of B mesons are an ideal probe to search for physics beyond the Standard Model (SM), since contributions from new particles can lead to effects that are of similar size as the SM predictions. The $B \to K^*\ell\ell$ decay involves the quark-level transition $b \to s\ell^+\ell^-$, a flavor-changing neutral current that is forbidden at tree level in the SM. Various extensions to the SM predict contributions, which can interfere with the SM amplitudes [1]. Global analyses of B decays hint at lepton-flavor non-universality, in which case muon modes would have larger contributions from new physics (NP) than electron modes [1, 2].

2. Angular Analysis

The $B \to K^\star\ell\ell$ decay can be described kinematically by three angles θ_ℓ, θ_K, ϕ and the invariant-mass squared of the lepton pair $q^2 \equiv M^2_{\ell\ell}c^2$. The angle θ_ℓ is defined as the angle between the direction of ℓ^+ (ℓ^-) and that opposite the B ($\bar{B}$) in the dilepton rest frame. The angle θ_K is defined as the angle between the direction of the kaon and that opposite the B ($\bar{B}$) in the K^* rest frame. Finally, the angle ϕ is defined as the angle between the two planes formed by the $\ell^+\ell^-$ system and the K^* decay in the B ($\bar{B}$) rest frame. The differential decay rate can be parametrized using definitions presented in Ref. [3] by

$$\begin{aligned}\frac{1}{\mathrm{d}\Gamma/\mathrm{d}q^2}\frac{\mathrm{d}^4\Gamma}{\mathrm{d}\cos\theta_\ell\,\mathrm{d}\cos\theta_K\,\mathrm{d}\phi\,\mathrm{d}q^2} = \frac{9}{32\pi}\Big[&\tfrac{3}{4}(1-F_L)\sin^2\theta_K + F_L\cos^2\theta_K + \tfrac{1}{4}(1-F_L)\sin^2\theta_K\cos 2\theta_\ell \\ &- F_L\cos^2\theta_K\cos 2\theta_\ell + S_3\sin^2\theta_K\sin^2\theta_\ell\cos 2\phi + S_4\sin 2\theta_K\sin 2\theta_\ell\cos\phi \\ &+ S_5\sin 2\theta_K\sin\theta_\ell\cos\phi + S_6\sin^2\theta_K\cos\theta_\ell + S_7\sin 2\theta_K\sin\theta_\ell\sin\phi \\ &+ S_8\sin 2\theta_K\sin 2\theta_\ell\sin\phi + S_9\sin^2\theta_K\sin^2\theta_\ell\sin 2\phi\Big], \end{aligned} \tag{2.1}$$

where the observables F_L and S_i are functions of q^2 only. The observables P'_i, introduced in Ref. [4] and defined as

$$P'_{i=4,5,6,8} = \frac{S_{j=4,5,7,8}}{\sqrt{F_L(1-F_L)}}, \tag{2.2}$$

are considered to be largely free of form-factor uncertainties [5]. Any deviation from zero in the difference $Q_i = P^\mu_i - P^e_i$ would be a direct hint of new physics [6]; here, $i = 4,5$ and P^ℓ_i refers to $P'_{4,5}$ in the corresponding lepton mode. The definition of P'_i values follows the LHCb convention [7].

3. Event Reconstruction

The four decay modes $B^0 \to K^{*0}\mu^+\mu^-$, $B^+ \to K^{*+}\mu^+\mu^-$, $B^0 \to K^{*0}e^+e^-$, and $B^+ \to K^{*+}e^+e^-$ are reconstructed, where the inclusion of charge-conjugate states is implied if not explicitly stated. In the reconstruction, the full $\Upsilon(4S)$ data sample recorded with the Belle detector [8] at the KEKB asymmetric-energy e^+e^- collider [9] is used that contains 772×10^6 $B\bar{B}$ pairs. A detailed description of the selection criteria for event candidates is given in Ref. [10].

The final classification for signal and background candidates is performed with a requirement on a neural network output for each B decay channel, where the network is trained using

event-shape variables, namely modified Fox-Wolfram moments [11], vertex fit information, and kinematic variables as input.

Signal and background yields are extracted with an unbinned extended maximum likelihood fit to the beam-energy constrained mass ($M_{\rm bc}$) distribution of $B \to K^* \ell^+ \ell^-$ candidates, presented in Fig. 1, where the signal is parametrized by a Crystal Ball function [12] and the background by an ARGUS function [13]. The signal shape parameters are determined from a fit to $B \to J/\psi K^*$ data in the corresponding q^2 veto region while the background shape parameters are allowed to float in the fit. In total, 127 ± 15 and 185 ± 17 signal candidates are obtained for the electron and muon channels, respectively.

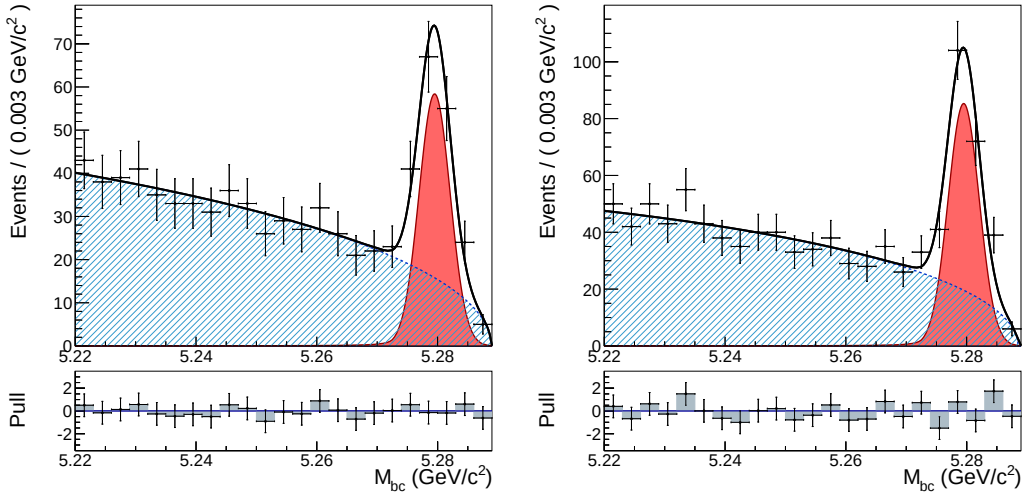

Figure 1: Distributions of the beam-energy constrained mass for selected $B \to K^* e^+ e^-$ (left) and $B \to K^* \mu^+ \mu^-$ (right) candidates. Background (shaded blue), signal (red filled) and total (solid) fit functions are superimposed on the data points

4. Fit Procedure

The analysis is performed in four independent bins of q^2, as listed in Table 1, with an additional bin in the range $1.0\ \mathrm{GeV}^2/c^2 < q^2 < 6.0\ \mathrm{GeV}^2/c^2$, which is favored for theoretical predictions [3]. To make maximum use of the limited statistics, a data-transformation technique [14, 15] is applied, simplifying the differential decay rate without losing experimental sensitivity. The transformation is applied to specific regions in the three-dimensional angular space, exploiting the symmetries of the cosine and sine functions to cancel terms in Eq. (2.1). With the following transformations to the dataset, the data are sensitive to the observable of interest:

$$P_4', S_4 : \begin{cases} \phi \to -\phi & \text{for } \phi < 0 \\ \phi \to \pi - \phi & \text{for } \theta_\ell > \pi/2 \\ \theta_\ell \to \pi - \theta_\ell & \text{for } \theta_\ell > \pi/2, \end{cases} \tag{4.1}$$

$$P_5', S_5 : \begin{cases} \phi \to -\phi & \text{for } \phi < 0 \\ \theta_\ell \to \pi - \theta_\ell & \text{for } \theta_\ell > \pi/2. \end{cases} \tag{4.2}$$

Following this procedure, the remaining observables are the K^* longitudinal polarization, F_L, the transverse polarization asymmetry, $A_T^{(2)} = 2S_3/(1-F_L)$, and P_4' or P_5'. Two independent maximum likelihood fits for each bin of q^2 are performed to the angular distributions to extract the $P_{4,5}'$ observables. The fits are performed using the data in the signal region of $M_{\rm bc}$ of all decay channels as well as separately for the electron and muon mode. The signal (background) region is defined as $M_{\rm bc} \geq 5.27$ GeV$/c^2$ ($M_{\rm bc} < 5.27$ GeV$/c^2$). For each measurement in q^2, the signal fraction is derived as a function of $M_{\rm bc}$. The background angular distribution is described using the direct product of kernel density template histograms [16] for ϕ, θ_ℓ and θ_K while the shape is predetermined from the above $M_{\rm bc}$ sideband. Acceptance and efficiency effects are accounted for in the fit by weighting each event by the inverse of its combined efficiency, which is derived from the direct product of the efficiencies in ϕ, θ_ℓ, θ_K and q^2. The individual reconstruction efficiency for each observable is obtained as the ratio between the reconstructed and generated Monte Carlo (MC) distributions.

5. Systematic Uncertainties

All methods are tested in pseudo-experiments using MC samples for each measurement and the results are compared to the input values. Systematic uncertainties are considered individually for all measurements if they introduce any angular- or q^2-dependent bias to the distributions of signal or background candidates. Non-negligible correlations between θ_ℓ and q^2 are found but not considered in the treatment of the reconstruction efficiency. The deviation between a fit based on generator truth and an MC sample after detector simulation and reconstruction reweighted with efficiency corrections is evaluated for a bias. The difference between the two fits is taken as the systematic uncertainty for the efficiency correction; this is the largest systematic uncertainty, ranging up to 43.9% of the statistical error with an average of 14.8% across all measurements. Peaking backgrounds are estimated for each q^2 bin using MC samples. In total, fewer than six (one) such background events are expected in the muon (electron) channels. The impact of the peaking component is simulated by performing pseudo-experiments with MC samples for signal and background according to the measured signal yields, replacing six randomly selected events from the signal class with events from simulated peaking background in each measurement. The observed deviation from simulated values is taken as the systematic uncertainty, which is on average 2.1% of the statistical error. An error on the background parametrization is estimated by repeating all fits with an alternative background description using third-order polynomials and taking the observed deviation as the systematic error. Resulting uncertainties range up to 36.5% of the statistical error with 8.5% on average. Finally, an error on the signal parametrization is considered by repeating the fit with the signal shape parameters varied by $\pm 1\sigma$, leading to systematic uncertainties of order 10^{-4}. Signal cross-feed is evaluated for all signal decay channels and found to be insignificant. The parametrization in Eq. (2.1) does not include a possible S-wave contribution under the $K^*(892)$ mass region. With the expected fraction of 5% [14, 7], we estimate the S-wave contribution for each measurement to be less than one event and the resulting effects to be negligible. Statistically equal numbers of B and $\bar{B}$ candidates in the signal window are found; consequently, *CP*-asymmetric contributions to the measured *CP*-even parameters are neglected. The total systematic uncertainty is calculated as the sum in quadrature of the individual values.

Table 1: Fit results for P_4' and P_5' for all decay channels as well as separately for the electron and muon modes. The first uncertainties are statistical and the second systematic.

q^2 in GeV$^2/c^2$	P_4'	$P_4^{e\prime}$	$P_4^{\mu\prime}$	P_5'	$P_5^{e\prime}$	$P_5^{\mu\prime}$
[1.00, 6.00]	$-0.45^{+0.23}_{-0.22} \pm 0.09$	$-0.72^{+0.40}_{-0.39} \pm 0.06$	$-0.22^{+0.35}_{-0.34} \pm 0.15$	$0.23^{+0.21}_{-0.22} \pm 0.07$	$-0.22^{+0.39}_{-0.41} \pm 0.03$	$0.43^{+0.26}_{-0.28} \pm 0.10$
[0.10, 4.00]	$0.11^{+0.32}_{-0.31} \pm 0.05$	$0.34^{+0.41}_{-0.45} \pm 0.11$	$-0.38^{+0.50}_{-0.48} \pm 0.12$	$0.47^{+0.27}_{-0.28} \pm 0.05$	$0.51^{+0.39}_{-0.46} \pm 0.09$	$0.42^{+0.39}_{-0.39} \pm 0.14$
[4.00, 8.00]	$-0.34^{+0.18}_{-0.17} \pm 0.05$	$-0.52^{+0.24}_{-0.22} \pm 0.03$	$-0.07^{+0.32}_{-0.31} \pm 0.07$	$-0.30^{+0.19}_{-0.19} \pm 0.09$	$-0.52^{+0.28}_{-0.26} \pm 0.03$	$-0.03^{+0.31}_{-0.30} \pm 0.09$
[10.09, 12.90]	$-0.18^{+0.28}_{-0.27} \pm 0.06$	-	$-0.40^{+0.33}_{-0.29} \pm 0.09$	$-0.17^{+0.25}_{-0.25} \pm 0.01$	-	$0.09^{+0.29}_{-0.29} \pm 0.02$
[14.18, 19.00]	$-0.14^{+0.26}_{-0.26} \pm 0.05$	$-0.15^{+0.41}_{-0.40} \pm 0.04$	$-0.10^{+0.39}_{-0.39} \pm 0.07$	$-0.51^{+0.24}_{-0.22} \pm 0.01$	$-0.91^{+0.36}_{-0.30} \pm 0.03$	$-0.13^{+0.39}_{-0.35} \pm 0.06$

6. Results

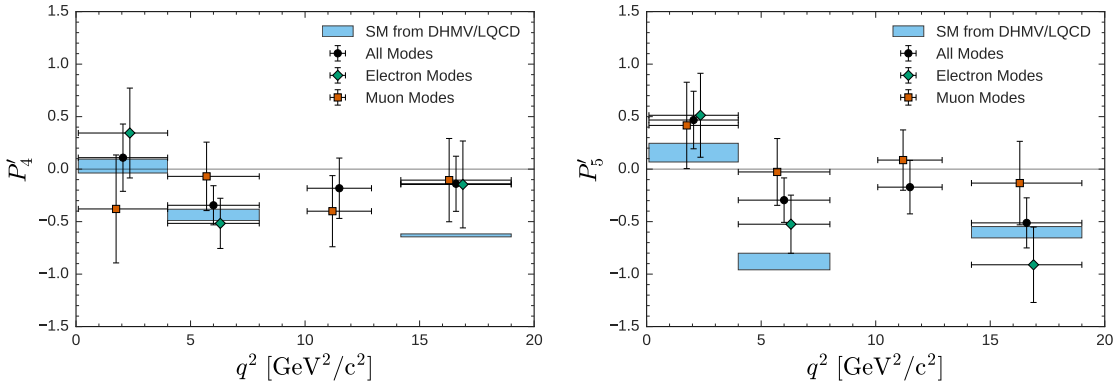

Figure 2: P_4' and P_5' observables for combined, electron and muon modes. The SM predictions are provided by DHMV [6] and lattice QCD [17] and displayed as boxes for the muon modes only (predicions for the electron modes vary slightly in the low-q^2 region). The central values of the data points for the electron and muon modes are shifted horizontally for better readability of the plot.

The result of all fits is listed in Table 1 and shown in Fig. 2 where it is compared to SM predictions by DHMV, which refers to the soft form-factor method of Ref. [18]. Predictions for the 14.18 GeV$^2/c^2 < q^2 <$ 19.00 GeV$^2/c^2$ bin are calculated using lattice QCD with QCD form factors from Ref. [17]. The predictions include the lepton mass, leading to minor corrections between the SM values for the electron and muon modes. For the former mode, fits in the region 10.09 GeV$^2/c^2 < q^2 <$ 12.90 GeV$^2/c^2$ are excluded because it overlaps with the $\psi(2S)$ veto range, leading to insufficient statistics for stable fit results. All measurements are found to be compatible with SM predictions. The strongest tension of 2.6σ (including systematic uncertainty) is observed in P_5' of the muon modes for the region 4 GeV$^2/c^2 < q^2 <$ 8 GeV$^2/c^2$; this is in the same region where LHCb reported the so-called P_5' anomaly [14, 7]. In the same region, the electron modes deviate by 1.3σ and all channels combined by 2.5σ (including systematic uncertainty). All measurements are compatible between lepton flavors. The $Q_{4,5}$ observables are presented in Table 2 and Fig. 3, where no significant deviation from zero is discerned.

7. Conclusions

In summary, we present the first lepton-flavor-dependent angular analysis measuring the observables P_4' and P_5' in the $B \to K^*\ell^+\ell^-$ decay. The observables $Q_{4,5}$ are also shown for the first

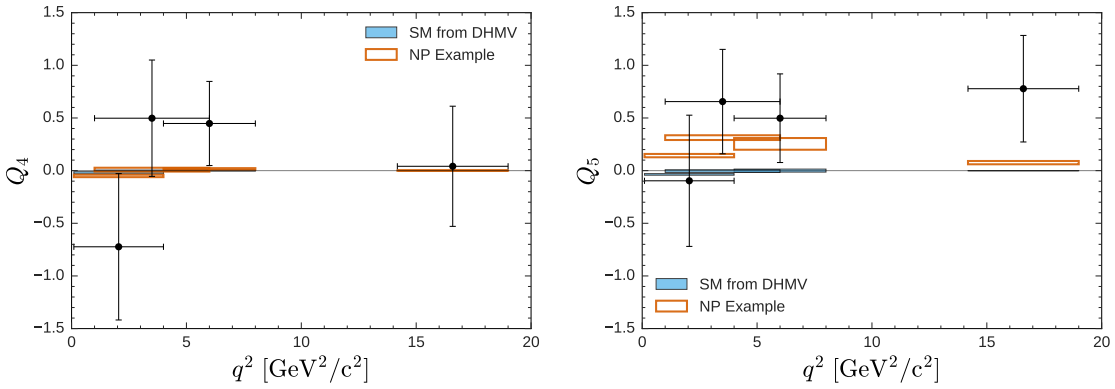

Figure 3: Q_4 and Q_5 observables with SM and favored NP "Scenario 1" from Ref. [6].

Table 2: Results for the lepton-flavor-universality-violating observables Q_4 and Q_5. The first uncertainty is statistical and the second systematic.

q^2 in GeV$^2/c^2$	Q_4	Q_5
$[1.00, 6.00]$	$0.498 \pm 0.527 \pm 0.166$	$0.656 \pm 0.485 \pm 0.103$
$[0.10, 4.00]$	$-0.723 \pm 0.676 \pm 0.163$	$-0.097 \pm 0.601 \pm 0.164$
$[4.00, 8.00]$	$0.448 \pm 0.392 \pm 0.076$	$0.498 \pm 0.410 \pm 0.095$
$[14.18, 19.00]$	$0.041 \pm 0.565 \pm 0.082$	$0.778 \pm 0.502 \pm 0.065$

time. Results are compatible with SM predictions, where the largest discrepancy is 2.6σ in P_5' for the muon channels. The results are now published in Ref. [10].

References

[1] Wolfgang Altmannshofer and David M. Straub. New physics in $b \to s$ transitions after LHC run 1. *Eur. Phys. J.*, C75(8):382, 2015.

[2] Sébastien Descotes-Genon, Lars Hofer, Joaquim Matias, and Javier Virto. Global analysis of $b \to s\ell\ell$ anomalies. *JHEP*, 06:092, 2016.

[3] Wolfgang Altmannshofer, Patricia Ball, Aoife Bharucha, Andrzej J. Buras, David M. Straub, and Michael Wick. Symmetries and Asymmetries of $B \to K^* \mu^+ \mu^-$ Decays in the Standard Model and Beyond. *JHEP*, 01:019, 2009.

[4] Sébastien Descotes-Genon, Joaquim Matias, Marc Ramon, and Javier Virto. Implications from clean observables for the binned analysis of $B- > K*\mu^+\mu^-$ at large recoil. *JHEP*, 01:048, 2013.

[5] Sébastien Descotes-Genon, Tobias Hurth, Joaquim Matias, and Javier Virto. Optimizing the basis of $B \to K^* \ell^+ \ell^-$ observables in the full kinematic range. *JHEP*, 1305:137, 2013.

[6] Bernat Capdevila, Sebastien Descotes-Genon, Joaquim Matias, and Javier Virto. Assessing lepton-flavour non-universality from $B \to K^* \ell\ell$ angular analyses. *JHEP*, 10:075, 2016.

[7] R. Aaij et al. Angular analysis of the $B^0 \to K^{*0} \mu^+ \mu^-$ decay using 3 fb^{-1} of integrated luminosity. *JHEP*, 02:104, 2016.

[8] A. Abashian et al. The belle detector. *Nucl. Instrim. Methods Phys. Res., Sect. A*, 479(1):117 – 232, 2002. Detectors for Asymmetric B-factories.

[9] S. Kurokawa and E. Kikutani. Overview of the kekb accelerators,. *Nucl. Instrum. Methods Phys. Res., Sect. A* **499***, 1 (2003)*, 1, 2003.

[10] S. Wehle et al. Lepton-Flavor-Dependent Angular Analysis of $B \to K^* \ell^+ \ell^-$. *Phys. Rev. Lett.*, 118(11):111801, 2017.

[11] S. H. Lee et al. Evidence for $B^0 \to \pi^0\pi^0$. *Phys. Rev. Lett.*, 91:261801, Dec 2003.

[12] Tomasz Skwarnicki. A study of the radiative CASCADE transitions between the Upsilon-Prime and Upsilon resonances. DESY-F31-86-02.

[13] H. Albrecht. Measurement of the polarization in the decay B $\to$ J/ψK *. *Physics Letters B*, 340:217–220, December 1994.

[14] R. Aaij et al. Measurement of form-factor-independent observables in the decay $B^0 \to K^{*0}\mu^+\mu^-$. *Phys. Rev. Lett.*, 111:191801, Nov 2013.

[15] M De Cian. *Track Reconstruction Efficiency and Analysis of $B^0 \to K^{*0}\mu^+\mu^-$ at the LHCb Experiment*. PhD thesis, University of Zurich, March 2013.

[16] Kyle S. Cranmer. Kernel estimation in high-energy physics. *Comput. Phys. Commun.*, 136:198–207, 2001.

[17] R. R. Horgan, Z. Liu, S. Meinel, and M. Wingate. Rare *B* decays using lattice QCD form factors. *PoS*, LATTICE2014:372, 2015.

[18] Sébastien Descotes-Genon, Lars Hofer, Joaquim Matias, and Javier Virto. On the impact of power corrections in the prediction of $B \to K^* \mu^+ \mu^-$ observables. *JHEP*, 12:125, 2014.